Article ID: 1003－6326(2003)05－1128－05

Computer simulation on primary α-phase of Al-7%Si solidification structure①

LI Rong-de(李荣德)[1], YANG Xiu-ying(杨秀英)[1], Li Run-xia(李润霞)[1]
LI Chen-xi(李晨曦)[1], LI Dian-zhong(李殿中)[2], LI Qiang(李 强)[2]
(1. School of Materials Science and Engineering,
Shenyang University of Technology, Shengyang 110023, China;
2. Institute of Metal Research, Chinese Academy of Sciences,
Shenyang 110016, China)

Abstract: Finite difference method was used to calculate the macroscopic transportation phenomena(including temperature and concentration fields) of Al-7%Si(mass fraction) alloy. On the basis of the results, coupled with local area magnification, the nucleation and growth of primary α-phase of Al-7%Si were simulated. Relating the growth process of α-phase of Al-7%Si alloy in space with structures of a sample section, the morphology and precipitating process of primary α-phase of Al-7%Si alloy was simulated. The results are in good agreement with those obtained experimentally.

Key words: Al-7%Si alloy; macroscopic transportation; primary α-phase; simulation
CLC number: TG 146.2 **Document code:** A

1 INTRODUCTION

The microstructure control during metal mould is a long-term research work, the previous research was based on the try-and-error method[1]. Since 1980's, the computer simulation method was used to study the formation of solidification microstructure and distortion structure. The computer-trial production may display dynamically the whole process of formation of solidification microstructure , or may predict the macro porous defects , and may optimize the process parameters through the approaches of numerical simulation cooperated with physical simulation .

In this paper, the authors established the model of 3-D equal dendrite growth of primary α-Al of Al-7%Si correlating with the structure of the section . It simulated the nucleation and growth processes of primary α-Al in 3-D space through establishing the macro-micro coupled mathematical model[2, 3] in which the heat, mass transportation in macroscope , nucleation and growth of crystal in microscope as well as the morphology of crystal of a section were integrated. A model connected microstructure formation and growth with macroscopic transportation (mass, momentum, energy, etc) is presented to complete the micro-macro scope uniform. The method is local area magnification[4] coupled with the finite difference method. The crucial areas were selected to be mesh with finer size when being micro-simulation, while the temperature and concentration fields belong to the macro scope still were applied to the whole casting. The method alleviates dramatically the contradiction between micro-simulation and great calculating capacity, and really reflects on the macro-micro mechanism of solidification .

2 EASTABLISHMENT OF MATHEMATIC MODEL

The model coupled the temperature, concentration fields in macroscope with the nucleation, growth model in microscope through mapping technology[5] and taking the local area magnification method .

2.1 Coupled model in solidification process

During the solidification of binary alloys, there occur the transportation of energy , mass, momentum. On the basis of volume average method proposed by Beckermann and Wang[6], the following assumptions were made:

1) Solid phase velocity is zero;

2) The heat balance can be achieved instantly on calculated cell;

3) There is local thermodynamic balance at the interface of solid-liquid;

4) Liquid phase solutes diffuse fully in a calculated cell.

At the same time, macro-transport model liquid is assumed to be impressible liquid. The physical properties of material in solid or liquid is independent of temperature. The approach is the Boussique approximatation, that is to say, except the gravity, there is no other force to make the liquid flow[7]. The ther-

① **Received date:** 2002－09－06; **Accepted date:** 2002－12－15
Correspondence: LI Rong-de, Professor, PhD; Tel: +86-24-25691688; E-mail: yangxiuying-y@163.com

mophysical parameters of Al-7% Si are listed in Table 1.

Dominated equation are described as follows:

Mixture mass conservation is

$$\frac{\partial}{\partial t}(\varphi_l \rho_l) + \nabla\cdot(\varphi_l \rho_l v_l) = -\frac{\partial}{\partial t}(\rho_s \varphi_s) \tag{1}$$

Liquid momentum conservation is

$$\varphi_l \rho_l \frac{\partial v_l}{\partial t} + \varphi_l \rho_l v_l \cdot \nabla v_l = -\varphi_l \nabla p + \nabla\cdot(\varphi_l \rho_l \eta_l \nabla v_l) + \nabla\cdot[\varphi_l \rho_l \eta_l (\nabla v_l)' + \rho_l \eta_l (v_l \nabla \varphi_l + \nabla \varphi_l v_l)] + v_l \frac{\partial}{\partial t}(\varphi_s \rho_s) - \varphi_s^2 \rho_l \eta_l K^{-1} v_l - \varphi_s \rho_l g \cdot [\beta_T (T - T_{ref})_T + \beta_C (c_t - c_{ref})_c] \tag{2}$$

Liquid mass conservation is

$$\varphi_l \rho_l \frac{\partial c_l}{\partial t} + \varphi_l \rho_l v_l \cdot \nabla c_l = \nabla\cdot(\varphi_l \rho_l D_l \nabla c_l) - \varphi_s \rho_s \frac{\partial c_s}{\partial t} + (c_l - c_s)\frac{\partial}{\partial t}(\varphi_s \rho_s) \tag{3}$$

Solid mass conservation is

$$\varphi_s \rho_s \frac{\partial c_s}{\partial t} = (c_l - c_s)\cdot\left|\frac{\partial}{\partial t}(\varphi_s \rho_s) + c_s \frac{\rho_s D_S}{l_s}\right| \tag{4}$$

Mixture energy conservation is

$$\varphi_s \rho_s \frac{dH_s}{dT}\frac{\partial T}{\partial t} + \varphi_l \rho_l \frac{dH}{dT} v_l \cdot \nabla T = \nabla\cdot[(\varphi_l \rho_l + \varphi_s \rho_s)\nabla T] - \varphi_s \rho_s \frac{dH_s}{dT}\frac{\partial T}{\partial t} + (H_l - H_s)\frac{\partial}{\partial t}(\varphi_s \rho_s) \tag{5}$$

where φ_l (φ_s) is the liquid (solid) volume fraction, ρ_l (ρ_s) is the density of liquid (solid) phase, v_l is velocity of fluid, p is pressure, T is temperature, η_l is the viscosity of liquid, K is the permeability in the mushy zone, β_T is coefficient of thermal expansion, β_C is coefficient of solute expansion, c_l (c_s) is concentration of liquid (solid) phase, D_L (D_S) is diffusivity of liquid (solid) phase, H_l (H_s) is the enthalpy of liquid (solid) phase, t is time, g is the acceleration of gravity, T_{ref} is reference temperature, and c_{ref} is reference concentration.

When liquid becomes solid, the solid parts will release latent heat. So the release of latent heat should be added to Eqn. (5). The equation of latent heat is

$$\frac{dH_s}{dt} = L\frac{\partial \varphi_s}{\partial t} \tag{6}$$

where L is latent heat.

The solid fraction in the liquid will change when liquid becomes solid, the equation can be dealt with as follow: $\varphi_s + \varphi_l = 1$.

$$\varphi_l = \begin{cases} 1, & T > T_l \\ \dfrac{T - T_s}{T_l - T_s}, & T_s \leqslant T \leqslant T_l \\ 0, & T < T_s \end{cases} \tag{7}$$

T_l and T_s represent the temperature of liquid and solid phases respectively on the phase chart. It is assumed that the solid and liquid compositions on the solid-liquid interface are in equilibrium. When the solidification on solid-liquid interface occurs, the solute partition between liquid and solid can be expressed as follows:

$$c_s^* = kc_l^* \tag{8}$$

where k is the partition coefficient, c_s^* and c_l^* are interface equilibrium concentrations in solid and liquid phases, respectively.

Through Eqns. (1)-(8), the results of temperature and concentration field can be obtained.

2.2 Micro-dynamic model

2.2.1 Nucleation model

During the cooling process, the local area magnification method was adopted to simulate the formation and evolvement of initial-Al phase. the macro different cells were meshed with equal size, then the results of temperature and concentration field achieved through mapping technology were given to the cell, finally, the nucleation and growth of cells were calculated.

To describe the heterogeneous nucleation[8] in the bulk liquid, the continuous nucleation model was adopted in which a Gaussian distribution of nuclei was considered. The nuclei density increase (d_n) was

Table 1 Thermophysical parameters of Al-7% Si alloy

Diffusion coefficient of solid /($m^2 \cdot s^{-1}$)	Specific heat of solid /($J \cdot kg^{-1} \cdot K^{-1}$)	Thermal conductivity in liquid /($W \cdot m^{-1} \cdot K^{-1}$)	Specific heat of liquid /($J \cdot kg^{-1} \cdot K^{-1}$)	Diffusion coefficicent of liquid /($m^2 \cdot s^{-1}$)	Thermal conductivity in solid /($W \cdot m^{-1} \cdot K^{-1}$)
10^{-12}	665.8	154.7	1 000	3×10^{-9}	167.8

Density /($kg \cdot m^3$)	Solidus temperature/ K	Liquidus temperature/ K	Latent heat/ ($J \cdot kg^{-1}$)	Partition coefficient	Initial solute/ %
2 665	850	891	3 719 446	0.117	7

induced by increase in the undercooling d(ΔT) according to the following Gaussian distribution:

$$n(\Delta T) = \frac{n_{max}}{\sqrt{2\pi}\Delta T_\sigma}\int_0^{\Delta T}\exp\left[-\frac{1}{2}\left(\frac{\Delta T-\Delta T_M}{\Delta T_\sigma}\right)^2\right]\mathrm{d}(\Delta T) \quad (9)$$

where ΔT_σ is the standard deviation, ΔT_N is the mean nucleation undercooling, and n_{max} is themaximum density of nuclei. The parameters of nucleation are listed in Table 2.

Table 2 Parameters of nucleation in bulk liquid

ΔT_N/K	ΔT_σ/K	n_{max}/m^{-2}
273.5	273.1	2.5×10^8

2.2.2 Growth model

The relationship between the growth velocity $v\{\Delta T(t)\}$ and the local undercooling $\Delta T(t)$ can be expressed as[9, 10]

$$v\{\Delta T(t)\} = k_1\Delta T(t)^2 + k_2\Delta T(t)^3 \quad (10)$$

where $k_1 = 2.9\times10^{-6}$ m/(s·k^2) and $k_2 = 1.49\times10^{-6}$ m/(s·k^3), for Al-7%Si alloy, respectively. α-Al is face-centered cubic, its preferential direction is ⟨100⟩ which is in accord with coordinates.

3 MORPHOLOGY AND PRECIPITATING PROCESS OF α-Al ON SECTION

It is very difficult to observe growth process of crystal[11-14] in space during experiment for the opacity of melt metal. The paper connects the precipitating process of crystals in space (shown in Fig. 1) with structures on a section to simulate the formation of microstructure[15].

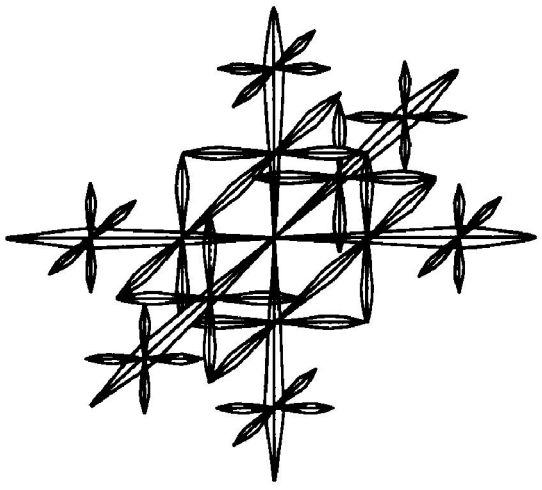

Fig. 1 Schematic of initial α-Al dendrite

3.1 Calculation of point of intersection between dendrite axis and sections

Supposing that the centre of α-Al dendrites lies on the origin O of 3-D right angle coordinates, and the initial dendrites grow along with the direction of x, y, z, then randomly section the dendrites. The point of intersection between the section with coordinates are P, Q, R, as shown in Fig. 2, $OP = x_0$, $OQ = y_0$, $OR = z_0$, then the plane equation is

$$\frac{x}{x_0}+\frac{y}{y_0}+\frac{z}{z_0} = 1 \quad (11)$$

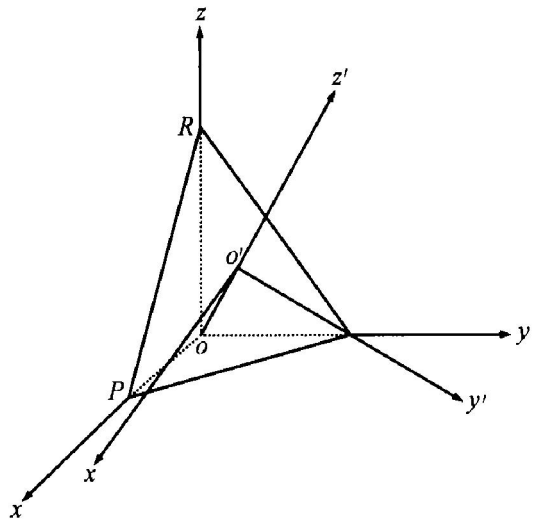

Fig. 2 Relative location of new and old coordinates

Turning Eqn. (11) into standard equation, it can be obtained:

$$Ax + By + Cz + D = 0 \quad (12)$$

where $A = y_0z_0$, $B = x_0z_0$, $C = x_0y_0$, $D = -x_0y_0z_0$

If vector is not equal to zero, $\boldsymbol{v} = \{m, n, p\}$, then the bee-line equation of dendrite axis which parallel to the vector $\boldsymbol{v}$ and overpass point $M_0(a, b, c)$ can be written as

$$\frac{x-a}{m} = \frac{y-b}{n} = \frac{z-c}{p} \quad (13)$$

The point of intersection between the dendrite axis and section must satisfy Eqns. (11), (12). Ordering that the specific value of Eqn. (13) is t, then it can be obtained:

$$x = a + ml,\ y = b + nt,\ z = c + pt \quad (14)$$

Derivation of Eqns. (13), (14) yields

$$(Am + Bn + Cp)t + (Aa + Bb + Cc + D) = 0$$

if $Am + Bn + Cp \neq 0$, then

$$t = -\frac{Aa + Bb + Cc + D}{Am + Bn + Cp} \quad (15)$$

Puting t into Eqn. (14), the point of coordinate between dendrite axis and the section can be obtained.

3.2 Coordinate transformation

There are nine angles between the old coordinates and the new one (seen Table 3) in the case that the origin of the new 3-D right angle coordinates lies in the plane π and the line between the origin of the old coordinates and the new ones are perpendicular to plane π and the axis z' of the new coordinate is along

with the direction of OO' (seen Fig. 2).

Table 3 Angle between new and old coordinates

New axis	Old axis		
	OX	OY	OZ
$O'X'$	α_1	β_1	γ_1
$O'Y'$	α_2	β_2	γ_2
$O'Z'$	α_3	β_3	γ_3

Supposing that origin O' of the new coordinate is point (a_0, b_0, c_0) on the old one, then it can be obtained:

$$a_0 = d\cos\alpha_3,\ b_0 = d\cos\beta_3,\ c_0 = d\cos\gamma_3 \quad (16)$$

The equation of transformation between the new coordinates and the old one is as follows:

$$\begin{cases} x' = (x - a_0)\cos\alpha_1 + (y - b_0)\cos\beta_1 + (z - c_0)\cos\gamma_1 \\ y' = (x - a_0)\cos\alpha_{21} + (y - b_0)\cos\beta_2 + (z - c_0)\cos\gamma_2 \\ z' = (x - a_0)\cos\alpha_3 + (y - b_0)\cos\beta_3 + (z - c_0)\cos\gamma_3 \end{cases} \quad (17)$$

where (x, y, z) is the point of the old coordinate, (x', y', z') is the point of the new coordinate.

If the value of coordinate of the point of intersection (x, y, z) between the dendrite axis of the old coordinate and the section is known, the value of coordinate (x', y', z') in the new coordinate can be calculated. For the points of intersection between the axis of dendrite axis and the section are on the same plane π, that is to say, on the new coordinate $z' = 0$, so after the coordinate is transformed by Eqn. (17), the point of intersection is $(x', y', 0)$. The essence of the transformation above-mentioned is to turn the 3-D coordinate of the point of intersection into the 2-D coordinate on the plane $z' = 0$. If we draw on the plane, then the real morphology of primary α-Al on a section can be obtained on the plane.

4 RESULTS AND VALIDATION

The sample was prepared as follows: the Al-7% Si alloy was put into the melting furnace, holded for 30 min, then coolled down at 0.6 ℃/s, when the temperature reached 585 ℃, sample was chilled into water. The samples were polished. Fig. 3 shows the process of nucleation, growth, dendrite arm coarsening of initial α-Al.

Fig. 3(a) infers that the nucleation of the initial phase and growth process of initial dendrite arm, Fig. 3(b) indicates the growth process of second dendrite arm, and Figs. 3(c), (d) mean that the second dendrite arms are coarsening. Fig. 4 shows the structure of a section through the chilling method when the temperature declines to 585 ℃ which is higher than eutectic temperature 577 ℃. The shape of the sectional structure is round, oval, rosettelike, which is consistent with the structure in Fig. 3. It can be imaginable that the shape of the dendrite in space should be the same as what is described in Fig. 1, in which the different sections will generate different shapes of structure as Fig. 4. Therefore the method we have adopted can reflect really the formation process of α-Al on a section.

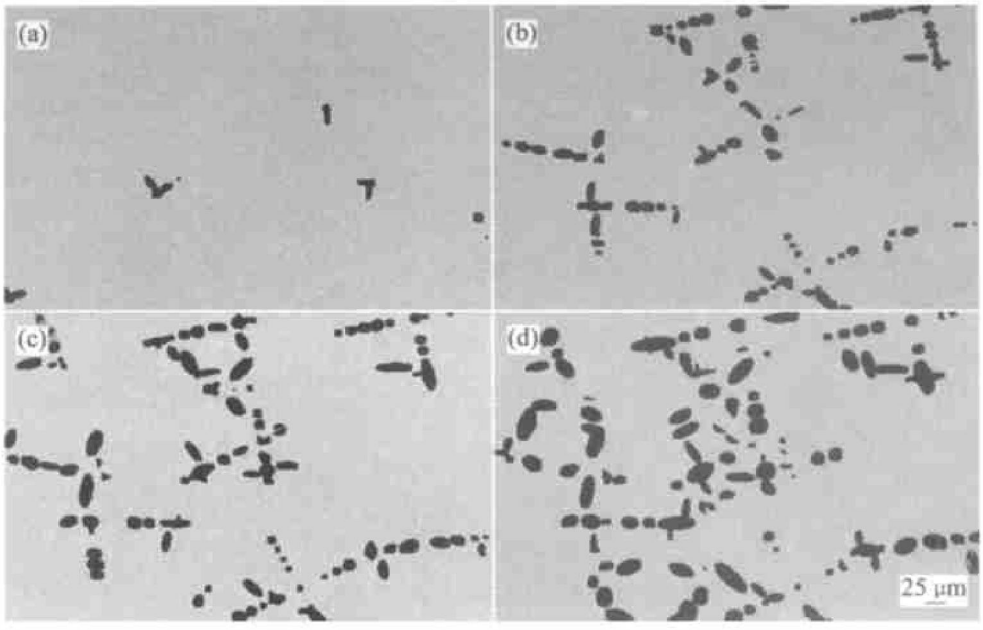

Fig. 3 Simulated precipitating process of α-Al dendrites on a section
(a) —10 s; (b) —40 s; (c) —50 s; (d) —83 s

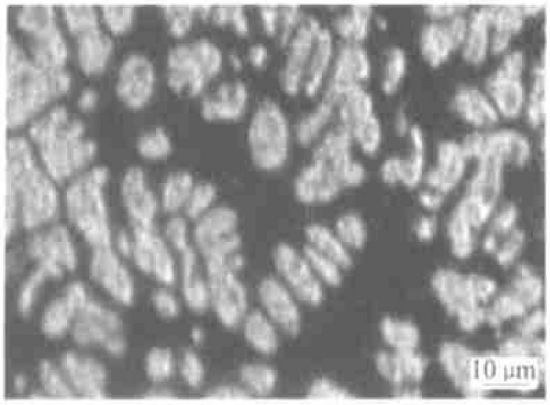

Fig. 4 Morphology of α-Al dendrites on section

5 CONCLUTIONS

1) The macro transportation process is simulated during solidification of Al-7% Si alloy, including temperature and concentration field, etc. The results show that temperature and concentration fieds of Al-7% Si alloy can be obtained by the simulation.

2) The macro-transportation phenomenon is connected with micro nucleation and growth process to simulate the microstructure of a section of initial phase. The results simulated are in good agreement with the experimental results.

REFERENCES

[1] LI Dian-zhong, ZHANG Yu-tuo, LIU Shi, et al. Modeling of material manufacturing process [J]. Acta Metall Sin, 2001, 37(5): 449 - 553. (in Chinese)

[2] LI Dian-zhong, ZHANG Yi, WANg Jun-qing . Mathematical model of equiaxed grains formation during solidification [J]. Foundry, 1994(10): 12 - 16. (in Chinese)

[3] LI Rong-de, MA Bing, XU Yu-qiao. Numerical method of solidification process in binary Al-Fe alloy under centrifugal casting[J]. Trans Nonferrous Met Soc China, 2000, 10(5): 614 - 618.

[4] WANG Tong-min, JIN Jun-ze. Local area magnification method for micro-modelling during solidification [J]. Metal Science & Technology, 1999, 7(7): 102 - 107. (in Chinese)

[5] WANG Tong-min. Research on the Micro-Modelling of Metal Solidification Process[D]. Dalian: Dalian University of Technology, 2000, 8. (in Chinese)

[6] Beckermann C, Wang C Y. Incorpo rating interfacial phenomena in solidification models [J]. JOM, 1994(1): 42 - 47.

[7] DU Qiang, LI Diang-zhong. Quantitative prediction of macrosegregation formation caused by natural convection during solidification of steel casting [J]. Acta Metall Sin, 2000, 36(11): 1197 - 1200. (in Chinese)

[8] Rappaz M, Gandin Ch A. Probabilistic modeling of microstructure formation in solidification processes [J]. Acta Metall Mater, 1993, 41(2): 345 - 360.

[9] Kurz W, Giovanola B, Trivedi R. Theory of microstructure development during rapid solidification [J]. Acta Metall, 1986, 34(6): 823 - 830.

[10] Zhu M F, Kim J M, Hong C P. Modeling of globular and dendritic structure evolution in solidification of an Al-7% Si alloy [J]. ISIJ Inter, 2001, 41(9): 992 - 998.

[11] Nastac L, Stefanescu D M. Macrotransport-solidification kinetics modeling of equiaxed dendritic growth (I) [J]. Metall Mater Trans, 1996, 27(A): 4075 - 4083.

[12] Nastac L, Stefanescu D M. Macrotransport-solidification kinetics modeling of equiaxed dendritic growth (2) [J]. Metall Mater Trans, 1996, 27(A): 4061 - 4074.

[13] Nastac L, Stefanescu D M. Simulation of microstructure evolution during solidification of Inconel 718 [J]. AFS Trans, 1996(193): 425 - 434.

[14] Stefanescu D M, Pang H. Modeling of casting solidification stochastic or dederministic [J]. Can Metall Q, 1998, 37(3/4): 229 - 240.

[15] LI Cheng-xi, SUI Zhi-tong, LI Yu-hai. Computer simulation on the precipitating process of perovskite phase from Ti-rich slag[J]. Acta Metall Sin, 2001, 37(7): 763 - 766. . (in Chinese)

(Edited by YANG Hua)